A Hybrid FDTD/Quasistatic Technique for the Accurate Modeling of RF Loss Mechanisms

E.T.K. Dalton and M.M. Tentzeris

Georgia Electronic Design Center, School of ECE, Georgia Institute of Technology,
Atlanta GA 30332-0269, USA
Fax: (404) 894-0222, email: edand@ece.gatech.edu

***Abstract* — This paper presents a novel method of coupling a quasistatic field solver with the finite-difference time-domain technique for the more efficient modeling of multilayer packaging structures including metal and dielectric loss effects. Lossy metal characteristics are first simulated with a dense quasistatic or a dense 2.5D-FDTD grid and the resulting field correction factors are then used to enhance the accuracy of a much coarser 3D FDTD mesh.**

I. Introduction

Significant attention is currently being devoted to the accurate modeling of packaged RF modules. Many of these structures involve multilayer dielectrics interspersed with layers of metallization [1]. These metals can be modeled as perfect electronic conductors, but for a large portion of RF structures, the finite nature of the metal thickness and conductivity play a significant role in device performance. Also, irregularities and structure details used in these geometries, including vias and wire bond connections, may be of a much smaller geometrical scale in comparison to the rest of the topologies.

The finite-difference time-domain (FDTD) technique [2,3] has long been employed due to its versatility in simulating high-frequency structures. However, as device features become smaller and integration increases, the computational load of a simulator experiences a corresponding increase. Since the Yee cell size is determined by the smallest feature of the simulation structure, and the number of cells is related to the total size of the structure, the computational domain quickly grows large. With the addition of non-ideal material parameters and with the incorporation of finite thickness and conductivity of metallization, the grid can become very large while the size of the time-step decreases, increasing the total simulation time. Static solutions have previously been considered as a method of reducing the computational overhead required for modeling discontinuous structures in FDTD [4,5], and for including imperfect material characteristics in the finite-difference method [6].

This paper presents the formulation of a hybrid FDTD method integrating a quasistatic field solver. This solver is first used to solve for static electric and quasistatic magnetic fields as highly accurate integral approximations. The output from the quasistatic solver can be used to determine the areas of highest field variation, and correction factors can be derived to account for inaccuracies caused by the use of a coarser dynamic (FDTD) grid. The static grid resolution is varied to determine what effect differences in the grids have on the accuracy of the simulations. Also used is a technique called "windowing", where the correction factors are thresholded and applied only in specific regions of the simulated structures, maintaining similar accuracy while significantly reducing computational requirements.

II. Hybrid Method Overview

The combination of the quasistatic solver and the FDTD method is an attempt to resolve some of the difficulties associated with modeling highly conductive thin materials in the time domain. Researchers often rely on heuristic approaches to generate the mesh for full-wave simulation, and this can result in inaccuracies in areas of large field variation [7]. The quasistatic solver is used in conjunction with a variable-gridded FDTD mesh to reduce errors in mesh size near structure discontinuities. The main advantage of the quasistatic solver is that, since it has no time-marching component, it does not take long to process, compared to a dynamic simulation of comparable resolution. In addition, it can be used as a preprocessing step that can optimize the grid size of the full-wave simulation.

For the integration of the quasistatic solver with the dynamic FDTD solver, correction factors for the electromagnetic fields in areas of high field variation are calculated. They improve the accuracy of the field solutions over the coarser dynamic grid through the solution of the integral forms of Ampere's and Faraday's laws, shown in (1) and (2), over a fine quasistatic grid.

$$\oint_l \vec{E} \cdot d\vec{l} = -\frac{d}{dt} \iint_A \mu \vec{H} \cdot d\vec{A} \tag{1}$$

$$\oint_l \vec{H} \cdot d\vec{l} = \frac{d}{dt} \iint_A \varepsilon \vec{E} \cdot d\vec{A} \tag{2}$$

The equations needed for the calculation of the correction factors are given in (3) and (4), where CF_l represents the line integral correction factor, CF_A represents the surface integral correction factor, and the Δ-terms represent the sizes of the FDTD coarse cells around which the integrals are discretized using the quasistatic values. The *dl*, *dx*, and *dy* variables of integration are the quasistatic grid sizes, which are much

smaller than the coarser FDTD cells. The F components in the numerators of the expressions are the field values derived from the quasistatic solver over the fine grid, and the F component in the denominator is the field value derived from the quasistatic solver in the same location as the field position on the FDTD coarse grid. The error can thus be reduced by using a very large number of quasistatic, fine-grid cells per dynamic, coarse-grid cells.

$$CF_l = \frac{\int \vec{F} \cdot d\vec{l}}{\overline{F} \cdot \Delta l} \tag{3}$$

$$CF_A = \frac{\iint \vec{F} \cdot d\vec{x} \cdot d\vec{y}}{\overline{F} \cdot \Delta x \cdot \Delta y} \tag{4}$$

Figure 1 shows a representation of the calculation for the surface integral correction factors. The coarse FDTD grid is displayed in the bolded dashed lines on the grid, and the fine quasistatic grid is shown by the fine black solid lines. In this case, the two grids are shown as uniform, with respect to both themselves and each other; however, this is not a requirement. The technique can be applied using variable gridding for both the fine and coarse grids. The dot at the center of the coarse FDTD cell denotes the location of the electromagnetic field used to calculate the dynamic cell field integral solution for use in (3) and (4).

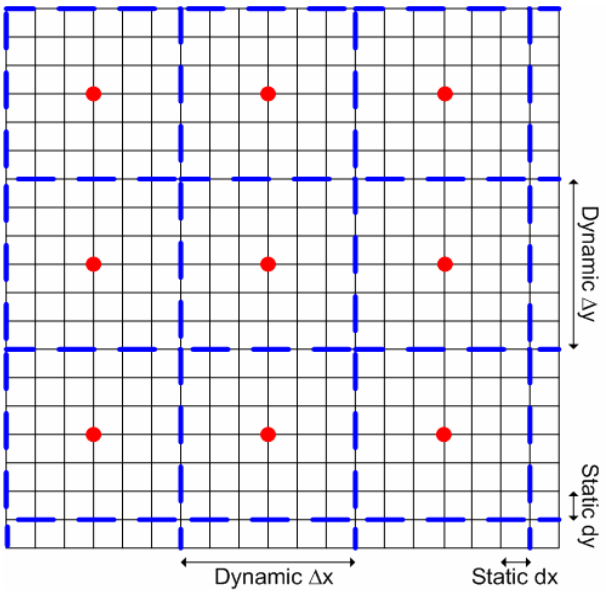

Fig. 1 Grid showing relationship of dynamic and static cells.

The surface integral is calculated to a very high degree of accuracy using the quasistatic solver over the fine grid, and, as shown in (4), this expression is used in the correction factor calculation. The coarse grid field integral approximation is determined by taking the quasistatic field value at the center of the dynamic grid cell and multiplying it by the area of the FDTD cell, or by the length of the cell, for line integral correction factors. These calculations are carried out over the entire grid, and are performed before the dynamic simulation, thus avoiding additional computational overhead. In areas of large field variation, the magnitude of the correction factors can be quite large.

Another method of deriving the correction factors for use in the FDTD update equations is by means of a very high resolution 2.5D FDTD simulation. This is the method that will be shown in this paper, as a proof-of-concept. The quasistatic technique and the application of the correction factors work in exactly the same way, but the application is more limited to a narrow frequency range.

Following the derivation of the FDTD update equations from the integral forms of Faraday's and Ampere's laws [2] and incorporating the correction factor terms in the formulation, the modified update expressions for H_x and E_x as shown in (5) and (6) are derived (conductivity terms and nonessential subscripts are omitted for simplicity):

$$E_x\big|_{j,k}^{n+1} = E_x\big|_{j,k}^{n} + \frac{2\Delta t}{\varepsilon \cdot CFA_{Ex}\big|_{j,k}} \cdot \left(\frac{CFL_{Hz}\big|_{j+.5,k} \cdot H_z\big|_{j+.5,k}^{n+.5} - CFL_{Hz}\big|_{j-.5,k} \cdot H_z\big|_{j-.5,k}^{n+.5}}{\Delta y} - \frac{CFL_{Hy}\big|_{j,k+.5} \cdot H_y\big|_{j,k+.5}^{n+.5} - CFL_{Hy}\big|_{j,k-.5} \cdot H_y\big|_{j,k-.5}^{n+.5}}{\Delta z} \right) \tag{5}$$

$$H_x\big|_{j-.5,k-.5}^{n+.5} = H_x\big|_{j-.5,k-.5}^{n-.5} + \frac{2\Delta t}{\mu \cdot CFA_{Hx}\big|_{j-.5,k-.5}} \cdot \left(\frac{CFL_{Ey}\big|_{j,k} \cdot E_y\big|_{j,k}^{n} - CFL_{Ey}\big|_{j,k-1} \cdot E_y\big|_{j,k-1}^{n}}{\Delta z} - \frac{CFL_{Ez}\big|_{j,k} \cdot E_z\big|_{j,k}^{n} - CFL_{Ez}\big|_{j-1,k} \cdot E_z\big|_{j-1,k}^{n}}{\Delta y} \right). \tag{6}$$

The relative orientations of the field components and the approximations of the integral equations are shown in Figure 2, which displays the contours and surfaces used in the solution of Maxwell's curl equations.

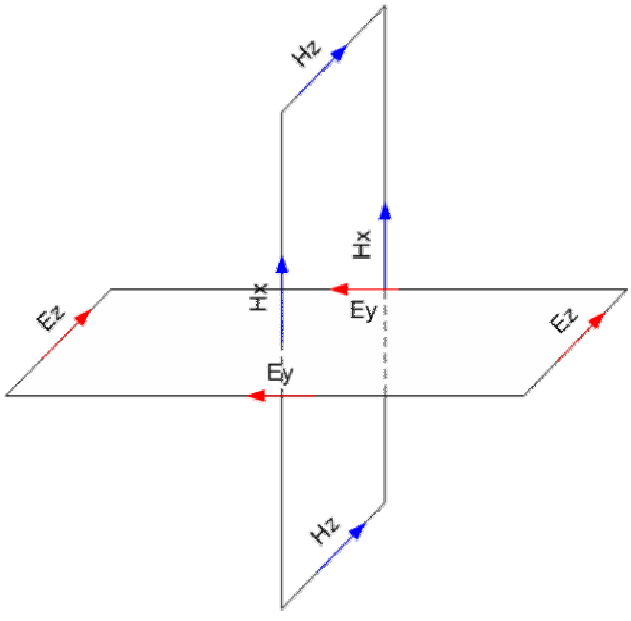

Figure 2: Faraday contour showing relation of fields for (6).

$$\Delta t = \frac{1}{\sqrt{\left(\frac{1}{\Delta x}\right)^2 4\left(CF_l^{\,y}\big|_{\max} \cdot CF_l^{\,z}\big|_{\max}\right) + \left(\frac{1}{\Delta y}\right)^2 4\left(CF_l^{\,x}\big|_{\max} \cdot CF_l^{\,z}\big|_{\max}\right) + \left(\frac{1}{\Delta z}\right)^2 4\left(CF_l^{\,x}\big|_{\max} \cdot CF_l^{\,y}\big|_{\max}\right)}} \quad (7)$$

The contour integral of the electric field is related to the surface integral of the magnetic field by Faraday's law. In this figure, the solved-for field is H_x, related to the loop including E_y and E_z. Equation (6) can be derived in a similar way.

In applying the correction factors derived from the quasistatic solver to the FDTD update equations, the stability of the hybrid algorithm is affected. A stability analysis gives a time step for the hybrid method which incorporates the effects of the correction factors. The calculation for the maximum time step is shown in (7), where dx, dy, and dz are the minimum sizes of the space discretization in each direction, and the $CF_l|_{max}$ are the maximum line integral correction factors over the entire grid derived from the quasistatic field solutions.

III. Preliminary Results

The above-described technique was benchmarked for a simple microstrip structure with thin finite-conductivity metal strips. Some preliminary results derived from these simulations are described in this section, including some comparisons of attenuation constants and characteristic impedance for the benchmarking structure, as well as evaluations of different correction factor "window" sizes.

Figure 3 illustrates the areas where the correction factors are significantly applicable (the "window" region mentioned previously) and shows the basic geometry for the test structure, a microstrip line on polyimide (ε_r=3.2) with a gold metallization (σ=3x10^7 S/m). The substrate thickness is 20 μm, with a strip height of 5 μm. Initially, the quasistatic solver was used for the whole structure and the dashed area was derived after thresholding the correction factor values and neglecting those in areas of low field variation.

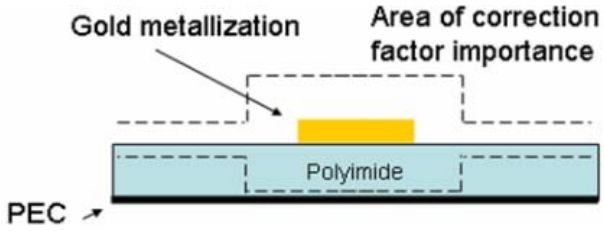

Fig. 3 Test structure geometry with indicated area of correction factor application

The test structure was first simulated using a very high resolution FDTD grid, for the comparison (below) with the quasistatic results. The high resolution grid size is 94 by 95 by 200 cells, with a minimum cell size of 200 nm, and uses 10 cells of PML absorber in all directions. It uses 25 cells for the 5μm strip thickness, and 20 cells for the 42 μm strip width. This number of cells is not, by itself, an extremely large load, but, due to the small size of the cells, the time step is also very small. This results in a very large number of time steps needed for convergence. In this case, over 400,000 time steps were needed, using an in-house developed parallel FDTD code on a 14-processor workstation cluster. The simulation time was approximately a day and a half.

The same structure was then modeled using the hybrid FDTD method and employing correction factors. Numerical simulations demonstrated that static cell sizes approximately half of a skin depth at the highest frequency of interest result in a calculation of the attenuation with acceptable accuracy. For practical cases, we apply this as a static grid resolution 10 times denser than the dynamic 3D FDTD grid with reasonable cell size, resulting in an approximate execution time economy of 1/6 to 1/7.

Figure 4 shows a comparison of simulation results using different window sizes, where the "window" is a region around the strip where the correction factors are expected to be significant, and are neglected outside that region (i.e., set equal to 1). In this case, the static mesh is approximately half of a skin depth for the strip metallization, which is a static cell resolution of 10x the dynamic cell resolution. It has to be noted that a window around the strip extended to 2 strip widths left and right is sufficient for the accurate modeling, while decreasing the number of cells that have to be treated with the correction factors by a factor 3-5. (The 'strip width' term refers to the width of the window on either side of the conducting strip.) The vertical window dimension is expanded along with the horizontal, approximately cell-for-cell.

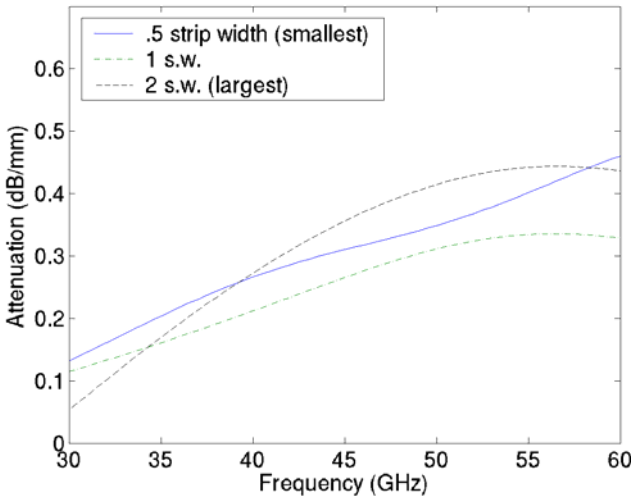

Fig. 4: Attenuation for different window sizes.

IV. Conclusion

In this paper, a method of coupling a quasistatic simulator with a conventional FDTD code for the purpose of improving accuracy while reducing simulation time through "subgridding" is presented. This is accomplished by the use of correction factors in the FDTD equations that can be derived from the quasistatic analysis of RF structures over a much finer grid with a cell size less than half of the skin depth in the metallized region. This technique can also be used to eliminate "guesswork" in meshing by determining areas of highest field variation from the magnitudes of the correction factors, something very important in the simulation of modern complex integrated RF modules, multilayer 3D RF front-ends or smart antenna arrays that include lossy dielectric and metal layers. A further reduction in the computational requirements can be achieved through the use of "windowing" techniques.

Acknowledgement

The authors wish to acknowledge the assistance of the Packaging Research Center at Georgia Tech, the Yamacraw Research Initiative of the State of Georgia, and NSF Career award #9984761.

References

[1] K. Lim, A. Obatoyinbo, A. Sutono, S. Chakraborty, C.-H. Lee, E. Gebara, A. Raghavan, J. Laskar, "A highly integrated transceiver module for 5.8 GHz OFDM communication system using multi-layer packaging technology," *2001 IEEE MTT-S Int. Microwave Symp. Dig.*, vol. 3, pp. 1739-1742, June 2001.

[2] K. S. Yee "Numerical solution of initial boundary value problems involving Maxwell's equations in isotropic media," *IEEE Trans. Antennas and Propagation*, Vol. 14, pp.302-307, 1966.

[3] A. Taflove and S. C. Hagness, Computational Electrodynamics: *The Finite-Difference Time-Domain Method*, pp.109-142, Artech House, Boston, 2000.

[4] D. B. Shorthouse and C.J. Railton, "The incorporation of static field solutions into the finite difference time domain algorithm," *IEEE Trans on Microwave Theory and Techniques*, Vol. 40, pp. 986-994, May 1992.

[5] C. J. Railton, D. B. Shorthouse, J. P. McGeehan, "Modelling of narrow microstrip lines using finite difference time domain method," *Electronics Letters*, Vol.28, pp. 1168-1170, June 1992

[6] M. Kunze and W. Heinrich, "3D hybrid finite-difference method for lossy structures based on quasi-static field solutions," *Proc. of the 2002 IEEE IMS*, pp. 1881-1884, Seattle, WA, June 2002

[7] T.I. Kosmanis, N.V. Kantartzis, T.D. Tsiboukis, "Accurate FDTD wavelet-Galerkin representation of field singularities near conductive wedges," *IEE Proc. Of Microwaves, Antennas and Propagation*, vol. 148, issue 3, pp. 163-166, June 2001.